Extended Abstracts of the 2012 International Conference on Solid State Devices and Materials, Kyoto, 2012, pp176-177

Effects of *in situ* Surface Passivation of AlGaN/GaN MOS-HEMT: A Simulation Study

S. S. Pannirselvam, Xinke Liu, Yee-Chia Yeo and Leng Seow Tan
Dept. of Electrical and Computer Engineering, National University of Singapore (NUS), 117576 Singapore
Phone: +65-6516-2563, Fax: +65-6779-1103 E-mail: eletanls@nus.edu.sg

1. INTRODUCTION

AlGaN/GaN heterostructure devices are very attractive for high power [1] and high frequency [2] applications. Advances in metal-oxide semiconductor high electron mobility transistor (MOS-HEMT) technology have led to low gate leakage current [3]. However, it is believed that surface-related charge trapping at the insulator/AlGaN interface limits the performance of AlGaN/GaN MOS-HEMTs [4]. It was shown recently that *in situ* passivation of this interface during fabrication can enhance the performance of the AlGaN/GaN MOS-HEMT. [5].

In this paper, TCAD simulations using SILVACO ATLAS was used to fit the experimental data in ref. 5 so as to study the effects of surface passivation on the experimentally fabricated AlGaN/GaN MOS-HEMTs.

2. EXPERIMENT OVERVIEW

The process flow for the experimentally fabricated $Al_{0.25}Ga_{0.75}N$/GaN MOS-HEMTs is shown in Fig. 1. The details of the fabrication process have been reported previously [5]. *In situ* vacuum anneal and SiH_4 gas treatment were used as the surface passivation technique. Fig. 2 shows the effects observed experimentally in passivated devices, compared to unpassivated devices, which did not undergo the passivation process. These effects were increase in the magnitude of the threshold voltage (V_{th}) (more negative), increase in the saturation drain current (I_{ON}), increase in extrinsic transconductance (g_m) and improvement in Sub-threshold Swing (*SS*).

3. SIMULATION

Fig. 3(a) shows the simplified cross-sectional device structure that was modelled in the TCAD simulation to match the experimental device. The polarization charge densities at the HfAlO/AlGaN, AlGaN/GaN and GaN/substrate were calculated using the equations reported by Ambacher et al. [6], together with Shimada's piezoelectric polarization model [7]. Fig. 3(b) shows the polarization sheet charge densities used in the simulations. In order to obtain a good fitting with the experimental V_{th}, the polarization charge densities in the simulation were reduced by ~15%, from the initial values calculated using Ambacher's equations [6], at the HfAlO/AlGaN, AlGaN/GaN and GaN/substrate interfaces. Thus, the polarization charge densities at the HfAlO/AlGaN, AlGaN/GaN and GaN/substrate interfaces were incorporated as -2.58×10^{13}, 1.04×10^{13} and 1.54×10^{13} cm^{-2} respectively in the simulation. This discrepancy between the theoretical and experimental devices can be attributed to inhomogeneities in the AlGaN/GaN heterostructure, interface roughness, possible overestimation of theoretical values, etc [8]. Fig. 3(c) shows the cross-sectional bandgap energy profile of the unpassivated device, under the gate electrode at zero gate bias. In this simulation, discrete deep donor-like traps (E_c – 0.37 eV) and discrete deep acceptor-like traps (E_v + 1.0 eV) were incorporated to represent the AlGaN surface defects due to nitrogen-vacancies and gallium-vacancies respectively [9][10].

In the simulation, low-field GaN mobility model reported by Albrecht et al. [11] and high-field GaN mobility reported by Farahmand et al. [12] were used.

4. RESULTS AND DISCUSSION

Fig. 4 shows the I_D-V_G plots for the unpassivated and passivated MOS-HEMT devices at V_{DS} = 5 V. The plots show a good fit between the experimental and simulated devices. The extracted V_{th} from the simulation are -4.12 and -4.78 V for the unpassivated and passivated devices respectively. These values are very close to the experimental V_{th} [5] (Table 1). Also, the increase in I_{ON} in the passivated device, for the same gate overdrive, could be due to increase in mobility because of decrease in carrier scattering. To achieve this close fitting, the donor-like trap densities in the unpassivated and passivated devices were set as 2.96×10^{13} cm^{-2}. Also, the simulation fittings show that the unpassivated device has an excess of 6.0×10^{12} cm^{-2} of acceptor-like traps compared to the passivated device. Therefore, the I_D-V_G plot fitting shows that the *in situ* passivation mainly reduced the acceptor-like traps in the HfAlO/AlGaN interface. Fig. 5 shows the transconductance (g_m)-V_G transfer characteristics for the unpassivated and passivated devices. These plots show good agreement between the experimental and the simulation results (Table 1). The extracted g_m peaks from the simulation for the unpassivated and passivated devices are 62.6 and 97.8 mS/mm respectively. This increase in g_m can be attributed to an increase in mobility due to reduction in carrier scattering.

Fig. 6 shows the conduction band and Fermi energy level under the gate electrode at zero gate bias. The reduction in the acceptor-like trap density results in a significant lowering of the energy band at the HfAlO/AlGaN interface. The triangular quantum well (Fig. 6 (inset)) at the AlGaN/GaN interface shows that the reduction of the acceptor-like trap density at the HfAlO/AlGaN interface also affects the energy band profile at the AlGaN/GaN interface. The calculated two-dimensional electron gas (2DEG) sheet carrier densities (n_s) at the AlGaN/GaN interface are 7.3×10^{12} and 8.5×10^{12} cm^{-2} for the unpassivated and passivated devices respectively. The calculated 2DEG n_s shows reasonable values with a difference of < 20% compared to the experimental devices, which were measured using room-temperature Hall measurement [5] (Table 1). Fig. 7 shows the log(I_D)-V_G plots for V_{DS} = 5 V in the sub-threshold region. The extracted values of the Sub-threshold Swing (*SS*) for the unpassivated and passivated devices from the simulation are 134.7 and 100.2 mV/dec, in good agreement with experimental values. Figure 8 summarises the observations that were made during this simulation study.

5. SUMMARY

This simulation study provides a plausible reason for the changes in the electrical characteristics of the passivated device compared to the unpassivated device. The *in situ* passivation process could have led to a reduction in the acceptor-like trap density at the insulator/AlGaN interface, which in turn results in enhanced performance of the passivated device.

Acknowledgement

The work is supported by the Defence Science and Technology Agency (DSTA), Singapore.

References

[1] Y.F. Wu, et al., *IEEE Trans. Elect. Dev.*, vol. 48, pp. 586, 2001.
[2] T. Palacios, et al., *IEEE Elect. Dev. Lett.*, vol. 27, pp. 13, 2006.
[3] Y. Yue, et al., IEEE Elect. Dev. Lett., vol. 29, pp. 838, 2008.
[4] R. Vetury, et al., *IEEE Trans. Elect. Dev.*, vol. 48, pp. 560, 2001.
[5] X. Liu, et al., *Appl. Phys. Lett.*, vol. 99, pp. 093504, 2011.
[6] O. Ambacher, et al., *J. Appl. Phys.*, vol. 87, pp. 334, 2000.
[7] K. Shimada, et al., *J. Appl. Phys*., vol. 84, pp. 4951, 1998.
[8] A. T. Winzer, et al., *Appl. Phys. Lett.*, vol. 86, pp. 181912, 2005.
[9] H. Hasegawa, et al., *J. Vac. Sci. Technol. B*, vol. 21(4), pp.1844, 2003.
[10] M. Miczek, et al., *J. Appl. Phys.*, vol. 103, pp. 104510, 2008.
[11] J. D. Albrecht, et al., *J. Appl. Phys.,* vol. 83 pp. 4777, 1998.
[12] M. Farahmand, et al., *IEEE Trans. Elect. Dev.*, vol. 48, pp. 535, 2001.

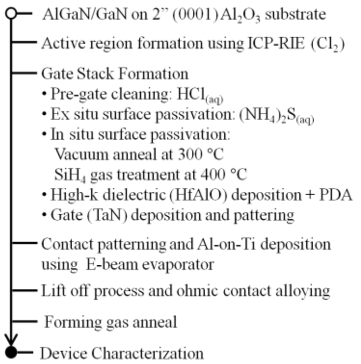

Fig. 1. Fabrication process flow of AlGaN/GaN MOS-HEMTs [5].

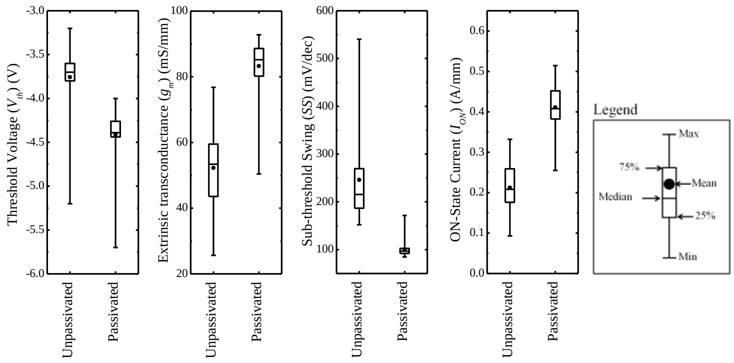

Fig. 2. Summary of experimental results observed in AlGaN/GaN MOS-HEMTs due to the *in situ* passivation. The *in situ* passivation resulted in (a) increase in V_{th} (more negative), (b) increase in g_m, (c) decrease in SS and (d) increase in I_{ON} [5].

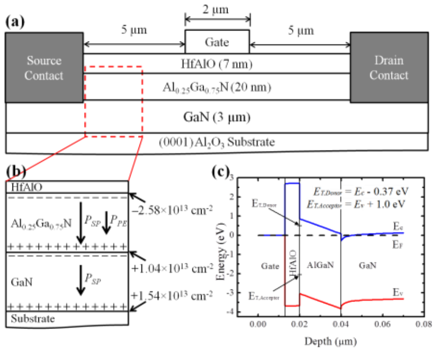

Fig. 3.(a) Cross-sectional schematic of simulated AlGaN/GaN MOS-HEMT structure. (b) Polarization sheet charges at HfAlO/AlGaN, AlGaN/GaN and GaN/substrate interfaces. (c) Bandgap structure of AlGaN/GaN MOS-HEMT showing the relative energy levels of the donor-like and acceptor-like traps.

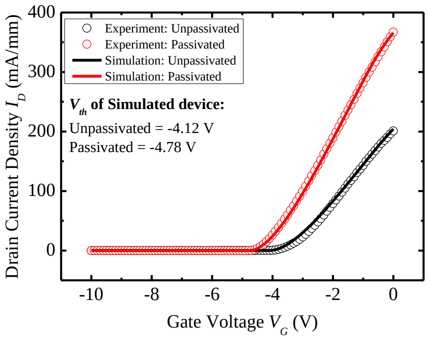

Fig. 4. I_D-V_G characteristics of unpassivated and passivated AlGaN/GaN MOS-HEMT at V_{DS} = 5 V for experimental [5] and simulated devices.

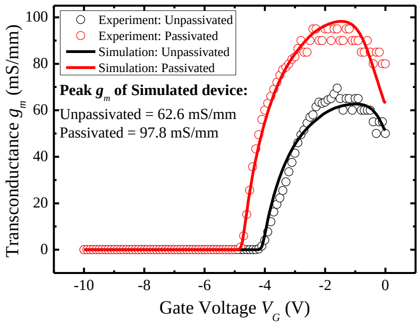

Fig. 5. g_m-V_G transfer characteristics of simulated and experimental [5] AlGaN/GaN MOS-HEMT at V_{DS} = 5 V. Peak g_m values for unpassivated and passivated devices (simulation) are 62.6 and 97.8 mS/mm respectively.

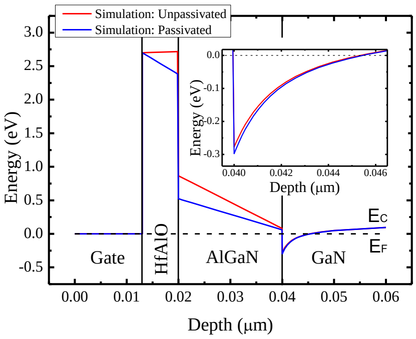

Fig. 6. Simulated conduction band alignment of unpassivated and passivated AlGaN/GaN MOS-HEMT devices. Triangular quantum at the AlGaN/GaN interface (inset).

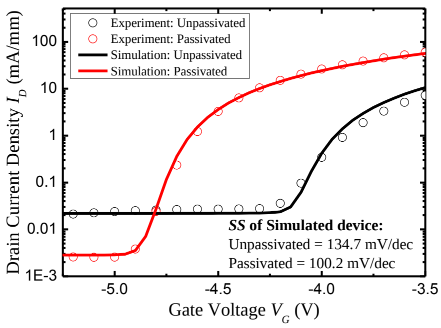

Fig. 7. Log(I_D)-V_G curves of simulated and experimental [5] AlGaN/GaN MOS-HEMT at V_{DS} = 5, near the SS region. SS values for the unpassivated and passivated devices (simulation) are 134.7 and 100.2 mV/dec respectively.

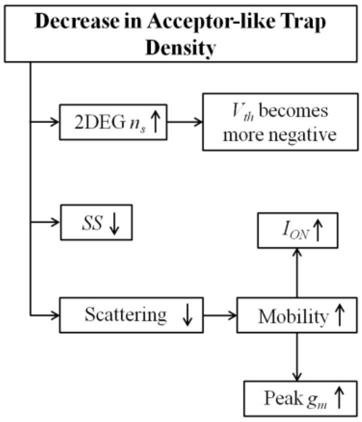

Fig. 8. Flow chart showing the summary of the studies performed using the TCAD simulation. Decrease in acceptor-like trap density leads to increase 2DEG sheet carrier concentration (n_s) at the AlGaN/GaN interface, and reduction in Sub-threshold Swing (SS) and carrier scattering. Increase in sheet carrier concentration (n_s) at AlGaN/GaN interface increases threshold voltage (V_{th}) (more negative). Decrease in carrier scattering increases mobility, which in turn increases ON-state current (I_{ON}) and transconductance (g_m).

Table 1: Comparison of experiment [5] and simulation V_{th}, n_s, peak g_m and SS.

	Experiment		Simulation	
	Unpassivated	Passivated	Unpassivated	Passivated
Threshold Voltage (V_{th}) (V)	-4.14	-4.77	-4.12	-4.78
2DEG Sheet Carrier Concentration (n_s)(cm⁻²)	0.86×10^{13}	1.04×10^{13}	0.73×10^{13}	0.85×10^{13}
Peak Transconductance (g_m) (mS/mm)	65.0	95.0	62.6	97.8
Sub-threshold Swing (SS) (mV/dec)	204.1	111.5	134.7	100.2